ALPHA FOUNDATION FOR THE IMPROVEMENT OF MINE SAFETY AND HEALTH

Final Technical Report

Project Title: Augmented Reality Proof-of-Concept Technology for Aiding Mine Rescue and Escape.

Grant Number: AFC820-54

Organization: Colorado School of Mines

Principle Investigator: Andrew J Petruska, PhD

Contact Information : Director: M3Robotics Lab
Department of Mechanical Engineering
Colorado School of Mines
161"0 Illinois St., Golden, Co 80401.
Phone: 303-384-2OZt,
Email: apetruska@mines.edu

Period of Performance: 36 Months, September 2019 - December 2023

This study was sponsored by the Alpha Foundation for the Improvement of Mine Safety and Health, Inc. (ALPHA FOUNDATION). The views, opinions and recommendations expressed herein are solely those of the authors and do not imply any endorsement by the ALPHA FOUNDATION, its Directors and staff.

1.0 Executive Summary

First responders face a myriad of challenges when searching for personnel in a disaster scenario. Possibly the most acute challenge is the complete lack of visibility owing to a combination of dust, smoke, and pitch-black conditions. Not only does the opacity of the air limit the responder's ability to navigate efficiently, but it also prevents responders from identifying a hazardous condition until in close proximity. Moreover, the complex environment compounds the difficulty of navigating and searching the area. Enhanced perception and localization technologies that enable rapid and safe disaster response could mitigate the mine rescue team's risk and reduce response times.

We provide these responders with situation awareness by lifting the veil of the conditions and providing them with an augmented reality display of the surrounding environment. By leveraging the LiDAR sensor and thermal camera, we constructed a 3D representation of the space in real-time. This is visualized on a lightweight wearable display, HoloLens, allowing the responders to see around their environment as if it were well-lit and smoke-free. Depending on the emergency setting (evacuation or search and rescue), visualization methods such as color, shape, etc. help responders in different ways.

(a)

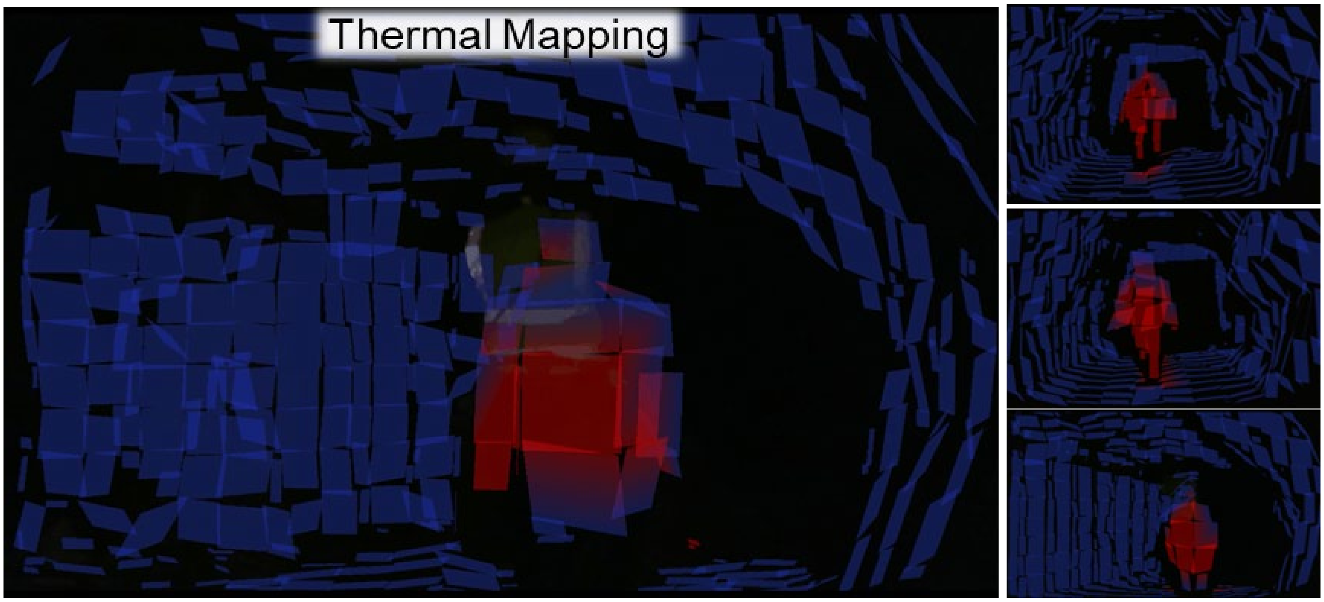

(b)

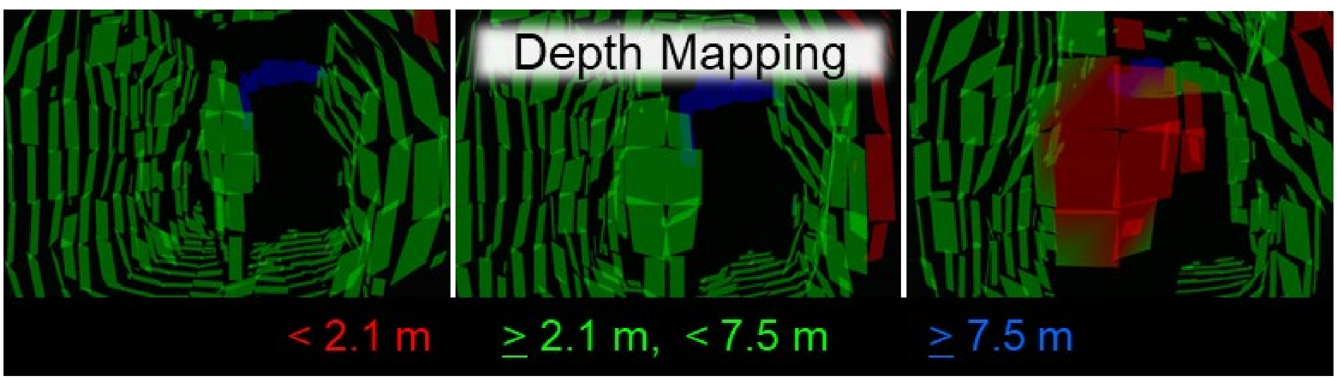

(c)

Figure 1: Visualization options of (a)single color mapping, (b) thermal mapping, (c) depth mapping.

The resulting system integrates LiDAR, Thermal Camera, and Microsoft HoloLens onto a wearable platform such as a hardhat and a belt or backpack. The processing and power storage are integrated into a waist-belt mounted package with a cap-lamp style cable connecting the two. This enables the user to look around with minimal impact on their motion.

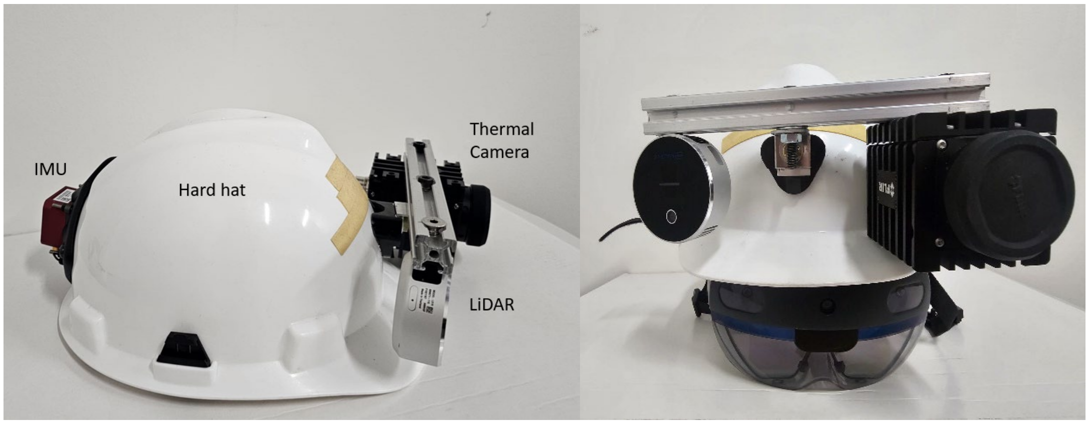

Figure 2: Integration of hardware: Thermal camera, LiDAR, IMU, and HoloLens on hard hat

The resulting system is tested internally and helps users navigate in a pitch-black underground mine tunnel in Edgar Mine. Initial results yield that for an evacuation scenario, depth mapping is more helpful than single color or thermal. On the other hand, for search and rescue missions, thermal camera yields faster response time from the users. To extend the usability and understand which visualization option is better, a user study is designed and gets the "IRB Exempt" status. Initial tests are conducted with five people in pitch-black tunnels with some obstacles and heat sources to mimic human presence. Figure 3 shows the training route.

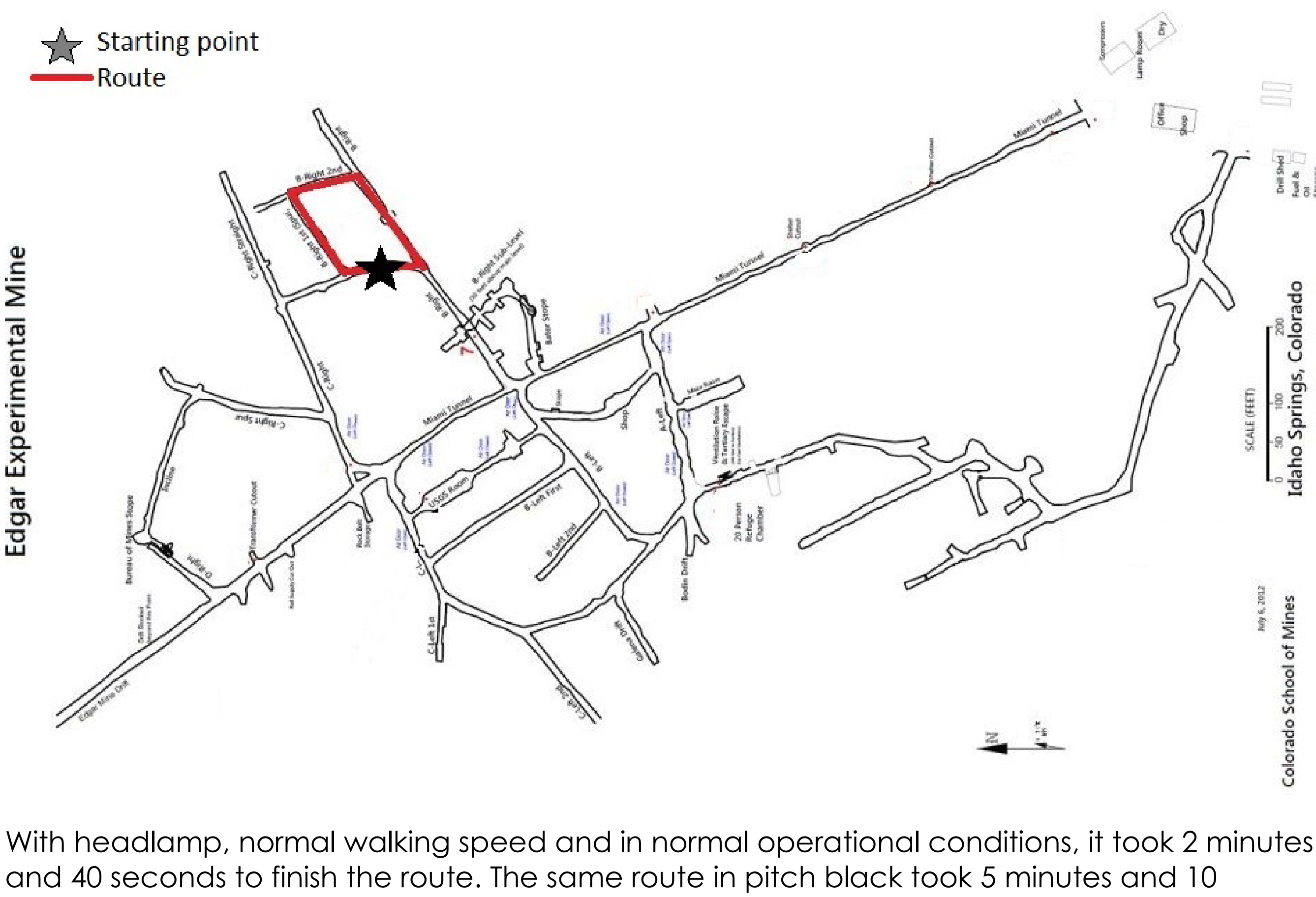

With headlamp, normal walking speed and in normal operational conditions, it took 2 minutes and 40 seconds to finish the route. The same route in pitch black took 5 minutes and 10 seconds on average. It should be noted that the test subjects have never been on this route before. They passed the route with the AR visual enhancement for the first time and then went with a headlamp. Moreover, these test subjects have only been in an underground mine less than 5 times in their entire life. Although additional subjects and tests needed to conclude a statistical results, we are optimistic that with our design even an untrained person can find their way out.

In the long run, the technology will enable faster, safer, and more effective disaster response for mine rescue operations. Not only will it allow the responders to search the environment more rapidly, but it will also enable them to detect unexpected hazards before they become imminent threats. Moreover, the utility of the developed system is far-reaching, for example, for first responders searching for smoke-filed burning structures. One day, it may also enable autonomous systems to navigate these occluded environments effectively and enable disaster response to focus on the rescue in search-and-rescue.

2.0 Problem Statement and Objective

After natural or man-made disasters, saving lives is a time-critical mission [1]. While racing with the clock, search and rescue teams tackle environmental difficulties [2]. One of the most challenging locations is subterranean spaces such as tunnels, mines, or caves. These locations are not only GPS-denied, but also have low to no visibility with uneven surfaces [3]. Moreover, due to its challenging nature, many devastating disasters occur in underground mines; hence, advanced indoor navigation solutions are needed [4]. In emergencies, the environment encountered by the mine rescue personnel is often visually occluded with dust and smoke to the point where visual perception is completely compromised, and the vision is restricted to 1-3 feet [5].

Traditional methods to guide emergencies in an underground mine include hand lines, pin-wheels, and strobe lights [6]. Using a green laser pointer, a more active approach has been shown to provide some situational awareness as its beam can penetrate the theatrical smoke enough to indicate the back and rib locations [5]. Another attractive option is thermal imaging, which can see through dust and smoke with the examples of firefighters and military operations where personnel traditionally use thermal imaging to assist with smoke-occluded situations [7].

In addition to seeing through dust and smoke, digital recreation of world in real time is another challenge not only in underground mine search and rescue operations, but also in the robotics community. After a tragic disaster, such as rock falls, roof collapse, or explosions, the underground map changes. Therefore, real-time 3D world construction is a necessity for safer and faster rescue operations [8]. The technology proposed to overcome this is an extension of the robotics area of simultaneous localization and mapping (SLAM) [9]. This approach uses sensor data to both reason on what the surrounding area looks like as well as where the sensors are in that area. SLAM solution has recently transitioned from the laboratory to the commercial sector; however, it is generally tested under ideal conditions, such as light and structured spaces [10]. Most SLAM methods rely directly on the data gathered either by making the data the ground truth and fitting directly to it (which is computationally expensive) or extracting landmarks and incorporating them into the model to reason on, which is less effective in underground environments [11]. Even with the recent advancement of sensor, battery, and processing power technologies, building an effective system that has the capability of seeing through pitch-black conditions with real-time world constructions has its limitations [12,13].

Recent advancements for mapping, navigation and object detection in underground environment were competed in the Defense Advanced Research Projects Agency (DARPA) Subterranean Challenge (SubT) in 2021 [14]. Although the main goal of the SubT was the autonomy of search and rescue robotics[15], DARPA pushes the limits of technologies that could be ready in 15 years and tries to make them happen in seven [16].

Underground search and rescue operations currently rely on humans and likely will for the near future as we look at the DARPA SubT challenge. Therefore, restoring visual information to first responders in emergency situations will enable them to search the environment more safely and more efficiently, as they will be able to scan an area for hazards, and will provide personnel with better situational awareness [17]. In this respect, augmented reality (AR) interfaces have great potential to leverage the search and rescue efforts in an emergency evacuation. Yet, the AR interface for real-time perception enhancement in underground mine search and rescue operations has not been explored sufficiently.

Given the shortfalls in mining operations, this work focuses on developing a hybrid human-machine system for solving situation awareness problems in pitch-black and smoke-filled underground mines. The proposed methodology is to combine thermal imaging, LiDAR, and AR. This aims to penetrate the smoke by leveraging thermal imaging while having real-time world construction with LiDAR and visualizing it on an AR device. By having this hybrid system, we aim to provide an AR image of the surrounding environment when pitch-black or visually occluded by smoke, dust, or other small particulates. This system is structured around an AR device, namely, Microsoft HoloLens, which will display an image to the user that depicts the surrounding environment in a meaningful way, but could be extended to any appropriate AR platform. This map enables the user to explore the environment with continuous improvements in fidelity as they maneuver. Lastly, the effectiveness of the proposed system is evaluated in an experimental underground mine.

Our study fills the necessity of having vision in pitch-black conditions during emergency evacuations in underground mines with a changing environment for search and rescue teams.

3.0 Research Approach

The real-time visual enhancement will enable the user to explore the environment with continuous improvements in fidelity as they maneuver. To accomplish this goal, a three-step approach is utilized.

1. Hardware: We tried to find the optimum hardware design by thinking about the effects on the agility of the users, power requirements throughout the escape route, and compatibility with each other.
2. Software: We built custom packages for each hardware to talk (publish and subscribe data stream) to each other by utilizing off-the-shelf software.
3. User Study: We aim to create an effective visualization of the voxelated spaces for users in an augmented reality setup. This aim shows how to do it effectively while avoiding information overload.

The steps show the evolution progress from proof of concept to prototyping to proof of use case scenario. Details of each step are given in sub-sections.

3.1 Hardware Design

This system is composed of multiple components and, as such, is run across various hardware. The hardware includes a NUC computer, Omnicharger, Krisdonia battery, hardhat, HoloLens, LiDAR, and thermal camera.

At the time of the hardware selection, there were two main AR device manufacturers, namely Magic Leap and Microsoft HoloLens. Both devices had their APIs and permits development mode. However Magic Leap was not allow to override of its built in light sensor [17] so that we choose Microsoft Hololens. Both thermal camera and LiDAR sensor is chosen based on their proven performance. Portable batteries, Omnicharger and Krisdonia, are chosen for their price performance and matching required output sockets. Descriptons and versions of each hardware is given in Table 1.

Table 1: List of Hardware

Hardware	Description	Version
AR Headset	Microsoft Hololens	1
LiDAR Sensor	Intel Real Sense	L515
Thermal Camera	FLIR	A70
Hardhat	OSHA compliant	-
Portable Battery	Omnicharger, Krisdonia	-
NUC	Portable Computer	Intel custom build

3.2 Software Design

The software include Linux, Windows, Unity, and Robot Operating System (ROS). Descriptions and versions are given in Table 2.

Table 2: List of Software

Software	Description	Version
Game Engine	Unity	2019.4.xxx
ROS	Robot Operating System	Melodic Morenia
Windows	Operating System	11
Ubuntu	Operating System	18.04

Sensor data collection in the form of LiDAR and thermal images collects and transmits 3D point data to scripts that manipulate and transform the data into another format by ROS bridge by NUK. Once the data has been converted, it is sent across a WebSocket on a local network to then be visualized in the Unity Editor and deployed into HoloLens. The images are color coded with thermal data. Unity is the development platform that allows the installation of the application on the HoloLens. Figure 3 shows a high-level overview of the data flow.

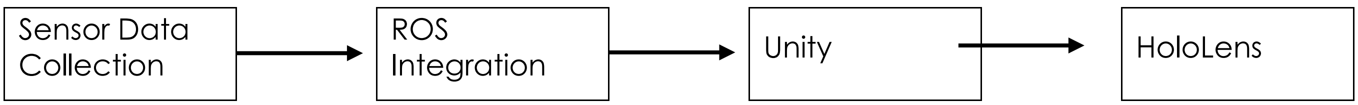

Figure 3: High level overview of the data flow

The sensors are required to be integrated into the C++/ROS application. The steps include creating a custom build image, developing a ROS node to parse incoming data, and customizing a startup script to configure the sensor data into HoloLens.

The main task for LiDAR integration is to develop a ROS node, a sub-application that runs within the main application, allowing the sensor fusion algorithm to incorporate with the post-processed data. Each of these packets contains data from one frame, where a frame is defined as the processed signals from a set of returned chirps. These values are collected for each frame and provide a snapshot of the sensor's current surrounding environment.

Another sensor data is coming from an IMU. This 9-axis inertial sensor is mounted to the backside of the helmet and the data stream is again fed from another ROS node to Unity. Ellipse-N INS from SBG Systems is utilized for its size, durable design, and highly accurate rotational accuracy. The device is calibrated and tested the sensor with its current ROS software driver to ensure its integration. It should be noted that not all ROS versions can facilitate these sensor flows. ROS Melodic Morenia is used in this study.

Lastly, a ROS node is developed to parse incoming data from the FLIR A70 thermal camera. This incoming data has been directly integrated into the visual stream to afford real-time pixel coloration according to temperature by ROS bridge to Unity.

Unlike a traditional operating system, ROS is a set of software libraries and tools that assist in building intercommunicative applications. This allows to freely communicate the point data between the LiDAR, thermal camera, Unity and HoloLens while also performing other computational tasks. A Linux machine was used to run the ROS network communication layer, process the positional point data and communicate it across a local network. A ROS network consists of nodes and topics. Nodes are executable scripts whereas topics contain the data being communicated. Nodes use this data in a sort of Subscription/Publication service. The ROS network that was implemented consists of several nodes and topics. The program that receives data from the LiDAR, IMU and thermal camera (/os1_node in Figure 2) publishes the topic "os1_cloud_node" which has a "point" component. This data is in the PointCloud2 Object (PCL2) format. Another node, "ouster_filte", subscribes to the "os1_cloud_node/points" topic and processes the point on LiDAR data, extracting x,y,z positions for each point and converts those positions into pixels of an image that is published to the "out_image topic". This is then sent across the rossbridge_websocket. Both the Unity Editor on the Windows machine and the HoloLens can then subscribe to this WebSocket to receive the image containing the positional data.

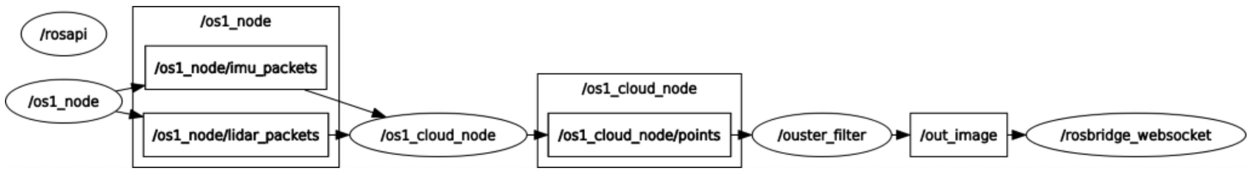

Figure 4 RQT Graph displaying a visual representation of the ROS network.

In Figure 4 ROS network is given. Nodes are circled, whereas topics are boxed. The arrows indicate the subscription/publication of data.

Similar to developing apps for a mobile device, developing an application on an AR device such as the HoloLens requires the use of an editor or development environment. As an emerging technology, AR development editors are quite limited. However, popular game development editors support the development of AR devices. As such, Unity is utilized for the visualization development of this application.

3.3 User Study

After finding optimum hardware and software combination, the last step is to find how to visualize the data stream as it is only numbers and letters. To solve this problem, we ask "What are the best ways and visual variables to visualize reconstructed data in augmented reality for first responders?" This question hypothesizes that AR interface with multi-colored reconstruction with depth data might help decrease response and assessment time, hence cognitive load. This will result in faster search and rescue operations.

Visual variables are one of the cornerstones of data visualization. The first categorization of visual parameters was proposed in 1967 by Bertin as size, color, orientation, texture, shape value (brightness), and position (dimensions on the plane) [18][19]. In addition to Bertin's visual variables, MacEachren suggested three more visual parameters: crispness, resolution, and transparency [20]. In 1994, Wolfe discussed the effects of complexity (referred to as cluttering) in visual search and the increase in cognitive load [21]. In 2014, Zhang et al. discussed the 2D visual variables compatibility and limitations in 3D visuals [22][23].

Similar to studies on 2D and 3D compatibility of visual parameters, VR and AR compatibility also needs to be investigated. Computer Human Interaction (CHI), one of the most prestigious [24] conferences in human-computer interaction, published a workshop paper at the CHI2021 conference as "Grand Challenges in Immersive Analytics." In this paper, the gaps were discussed by 24 different groups of professionals in their fields of expertise. The researchers pointed out 17 current key challenges and gaps for the future of the research field. These challenges can be sorted into four different categories, namely, "spatially situated data visualization," "interacting with immersive analytics systems," "collaborative analytics," and "user scenarios and evaluation" [25]. As stated under spatially situated data visualization, designing guidelines for visualization and understanding human senses and cognition in situated contexts are among the two challenges. Inappropriate usage of visual variables might result in users' misinterpreting critical data [26].

Laha et al. studied the effects of visual variables of head tracking, field of regard and stereoscopic rendering for volumetric data interpretation. They found that field of regard has a positive impact on tasks but other parameters have mixed effects [27]. Adams et al. studied shadow/shadowless and position (floating/grounded) variables for the depth perception of users in augmented reality. They found that current devices make users underestimate the distance regarding the visual variable but the position of the object and the shadow influence users' decisions [28]. Arjun et al. evaluated the effects of size, orientation, opacity, and shape for chart data understanding. They found that accuracy is affected the most by size and color. Moreover, cognitive load is affected the most by size, opacity and brightness [29].

A saliency map ©s a computer vision term that highlights visually striking parts of the image for the human eye, which was first proposed by Koch and Ulman [30] and implemented by Itti et al. [31][32]. Although many variations of saliency mapping algorithms exist, from a high-level perspective, these algorithms consider visual features including but not limited to color, orientation, location, and edges [33], and create a 2D image that represents the predictions of human eye movement [34]. For viewpoint selection, visualization, learning, assessment, and monitoring, keeping the correct saliency is essential [35][36]. Failure to develop correct salient regions in visualization might result in increased cognitive load, distraction, and overlooking critical data [37][38][39][40].

Since emergency response is a time-critical mission, appropriate visualization needs to be employed. Our aim is to investigate and benchmark visual variables for underground augmented reality visual enhancement.

Initial tests are done internally with the research team and human subject research design is submitted to the institutional review board. The application is approved as exempt study under 45 CFR 46.104(d)(3) (July 19, 2018) - https://www.ecfr.gov/on/2018-07-19/title-45/part-46/section-46.104#p-46.104(d)(3)

3.3.1 Initial Tests

Participants signed an informed consent form prior to the study. Participants then filled the background questionnaire that captured their experience with AR and underground mining. After the background questionnaire, we introduced the hardware and explained the experiment. Training route is given in Figure 7. We then gave a quick training on underground mining, equipment, and safety. After finishing the AR experiment we asked them the post survey questions which is given in Appendix A.

We recruited 5 voluntary participants for our study. There were 1 female and 4 males with ages ranging from 21 to 30. Only 2 of the participants self-reported having previous AR experience but not regular users. All participants had been in an underground mine before but not more than 5 times. They self reported that they have never been in the training route of the mine before.

We analyzed the results based on both quantitative and qualitative approaches. For the quantitative analysis, we considered participants' total time travel and the ability of noticing hot objects (humans, cross sections. For the qualitative analysis, we took users' responses to the post questionnaire into account.

Quantitative analysis yields finishing the route in 2 minutes and 40 seconds versus 5 minutes and 10 seconds in average with head lamp and AR enhancement, respectively.

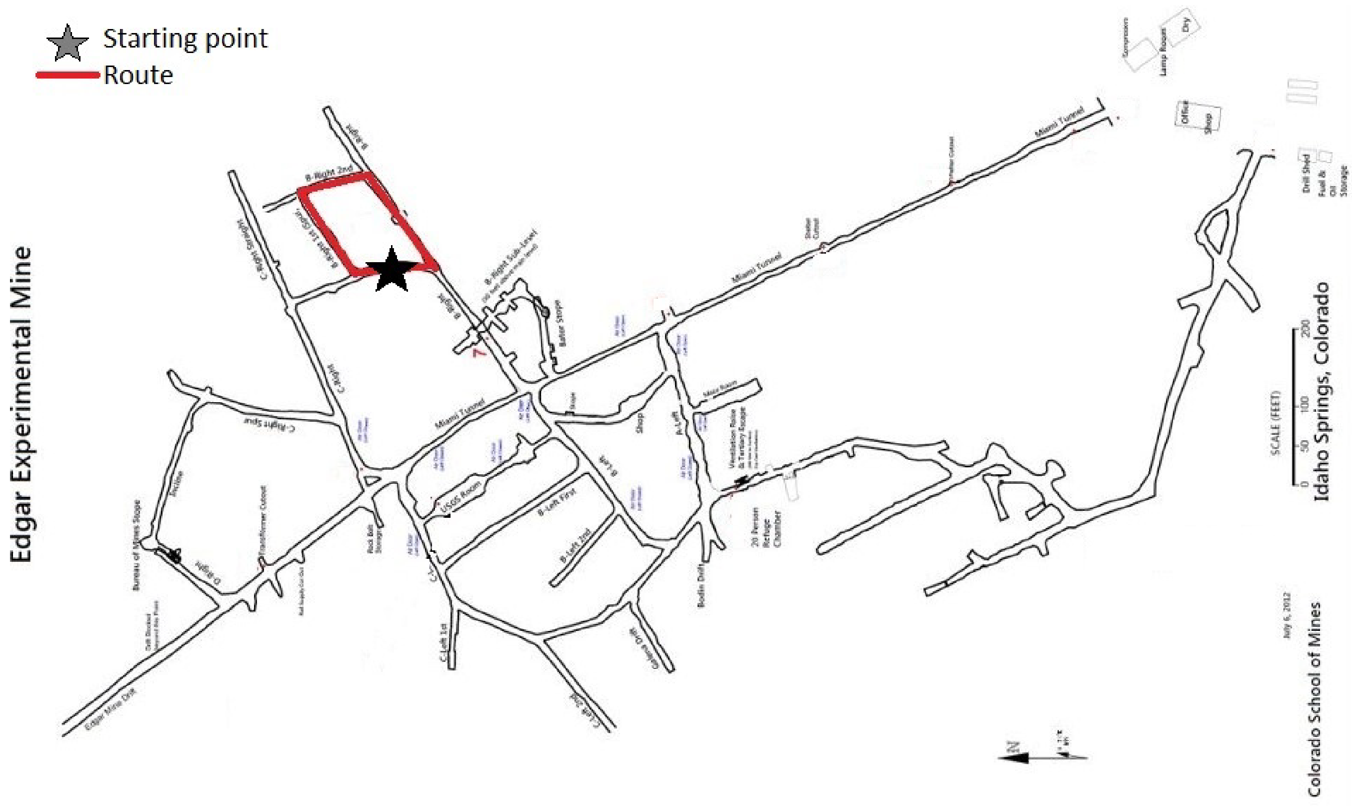

Figure 7: Training route

To be noted that the tests are done in pitch black conditions. We test the route with heavy smoke fill (hard to breathe) and thin smoke (cannot see with headlamp but can breathe). Figure 8 shows a snapshot of the tunnel with heavy smoke and thin smoke and how they appear in AR glasses.

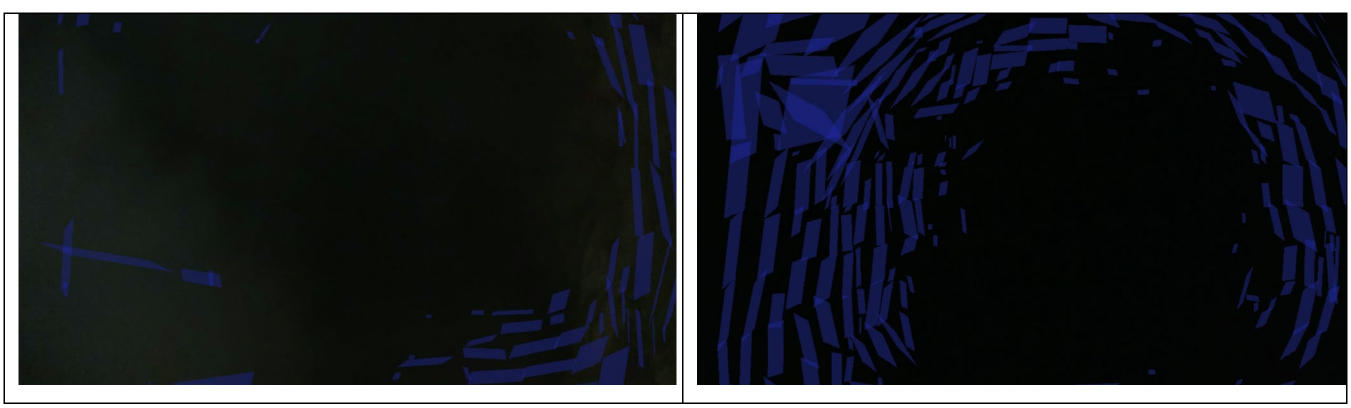

a) Heavy Smoke	b) Thin smoke

Figure 8: Heavy smoke and thin smoke snapshots

For the qualitative analysis, we asked the NASA Task Load Index (TLX) questions (Appendix A) to measuring a subjective mental workload assessment. It rates performance across six dimensions to determine an overall workload rating. The six dimensions are as follows:

1. Mental demand: how much thinking, deciding, or calculating was required to perform the task.

2. Physical demand: the amount and intensity of physical activity required to complete the task.

3. Temporal demand: the amount of time pressure involved in completing the task.

4. Effort: how hard does the participant have to work to maintain their level of performance?

5. Performance: the level of success in completing the task.

6. Frustration level: how insecure, discouraged, or secure or content the participant felt during the task.

Users are self reported their scores ranging between 1 to 21. Mental demand results are ranging 17 to 21, physical demand results are ranging between 15 to 21, temporal demand results are ranging between 15 to 21 effort results are ranging between 16 to 21, performance results are ranging between 11 to 19 and lastly the frustration results are 21 for all participants.

To sum up; although we can not have enough participants to conduct a statistical analysis, the research findings and conclusions are given in Chapter 4 and Chapter 6 respectively.

4.0 Research Findings and Accomplishments

The resulting system integrates LiDAR, IMU, Thermal Camera, and Microsoft HoloLens onto a wearable platform such as a hardhat and a belt or backpack. The processing and power storage are integrated into a waist-belt mounted package with a cap-lamp style cable connecting the two. This enables the user to look around with minimal impact on their motion.

Initial results yield possible visualization varieties. These visualization options are given in Figure 4 as a) single color mapping, b) thermal mapping, c) depth mapping.

(a)

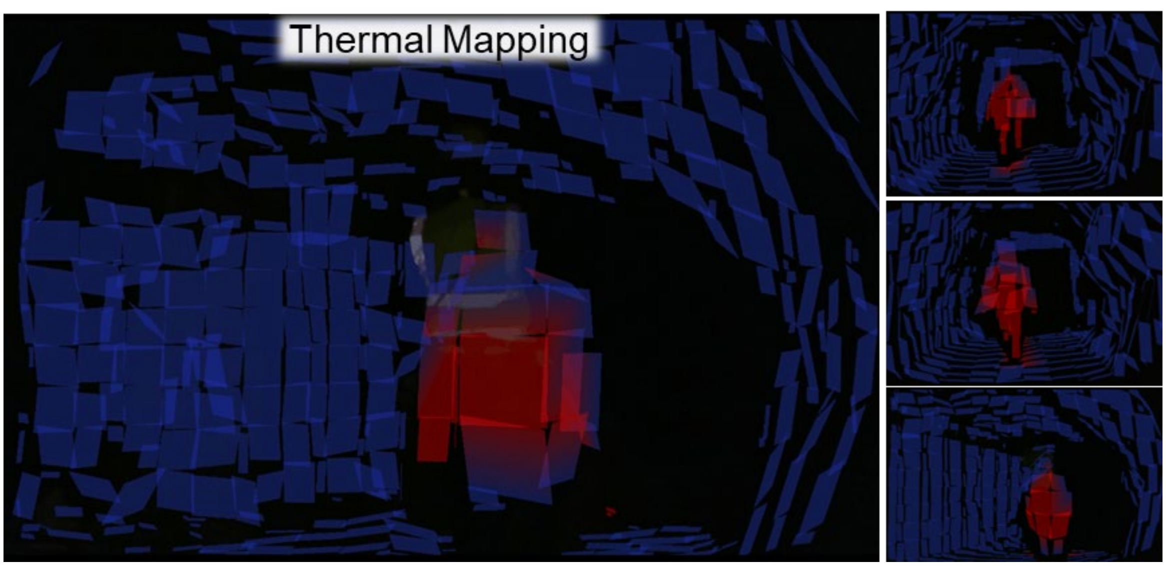

(b)

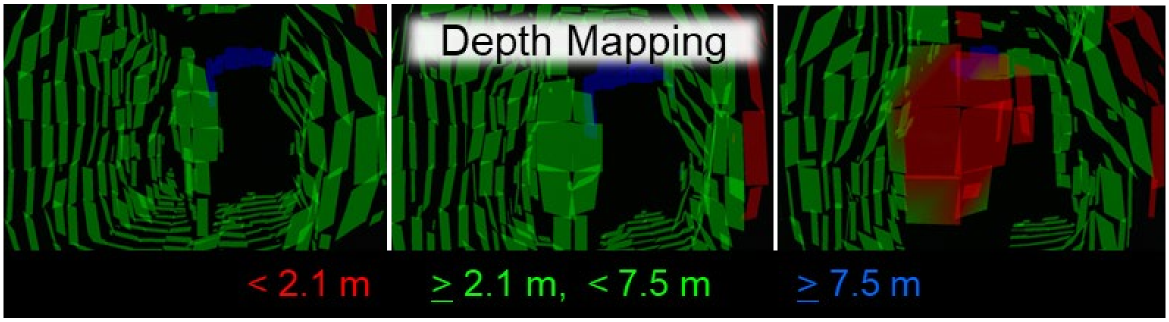

©)

Figure 5: Visualization options of (a)single color mapping, (b) thermal mapping, (c) depth mapping.

Among the visualization options, depth mapping with a thermal camera yields the most robust results. Color schemes to provide depth perception information are added as a user option, where red schemes indicate closer objects and green schemes indicate farther objects (Figure 5).

The display capabilities of the system have been expanded to include several different shapes that have tradeoffs in terms of both point density and fidelity. Each of these display variants can be generated directly from the Octree data and evaluated as one of the following:

1) Triangulated mesh, where the point-cloud is taken and the gd3 algorithm from the point-cloud library [41] is used to generate a tessellation,
2) Square surface patch, where the point cloud is packed into the Octree that tracks a Gaussian representation of the points measured in each voxel. A square patch is then generated that represents the average surface for that voxel,
3) Triangle surface patch, where the point cloud is packed into the Octree that tracks a Gaussian representation of the points measured in each voxel. A triangular patch is then generated that represents the average surface for that voxel,
4) Cube occupancy grid, where the point cloud is packed into the Octree, and the voxels that contain points are extracted and displayed to the user,
5) Cuboid surface representation, where the point cloud is packed into the Octree that tracks a 3D Gaussian representation which is converted into a rotated and scaled cuboidal shape,
6) Ellipsoid surface representation, where the point cloud is packed into the Octree that tracks a 3D Gaussian representation which is converted into an ellipsoid according to the standard deviations in each direction for display.

The number of vertices and triangles with 2D performance of each display type is given in Table 3.

Table 3: Display types with their respective number of vertices and triangles, and performances.

Display Type	*Number of Vertices*	*Number of Triangles*	*Qualitative 2D performance*	*Visualization*
Triangulated mesh: Triangle tessellation using gd3. Provides a smooth surface but is unpredictable between scans.	1,253	1,671	Poor-Good	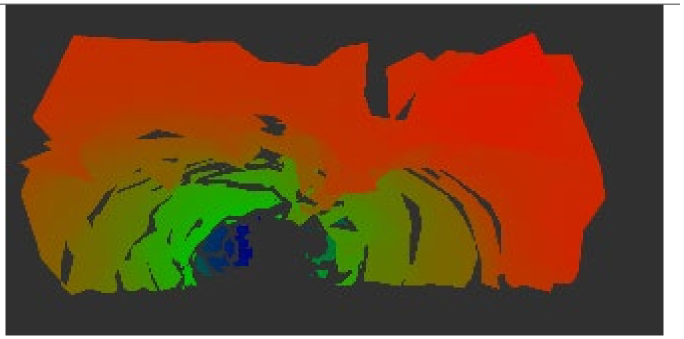
Square Surface Patch Square surface representation requires minimal triangles and vertices and provides a reasonable level of fidelity.	996	1,992	Good-Excellent	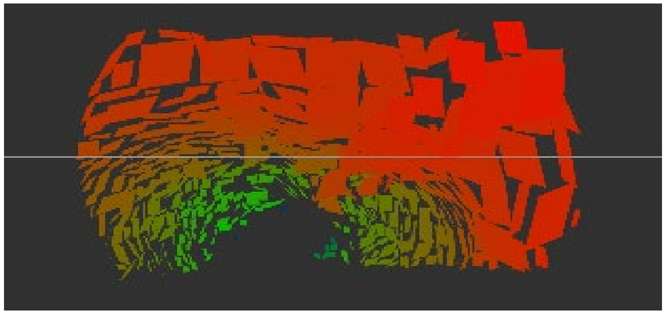
Triangle Surface Patch Triangle surfaces minimizes the number of triangles to send and voxels, but is disconnected and only provides moderate fidelity.	476	1,428	Good	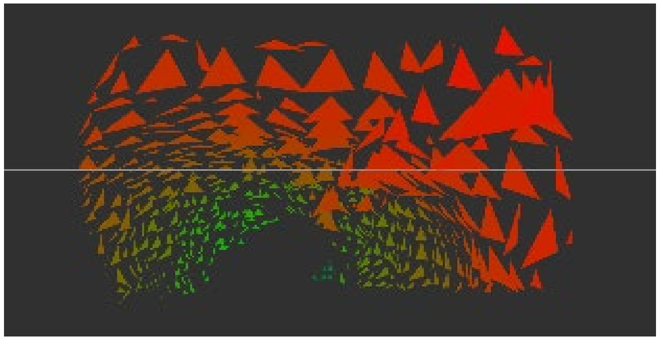

Cube Occupancy Grid: Cube occupancy. Very consistent but overly conservative and blocks much of the view.	5,712	3,808	Poor	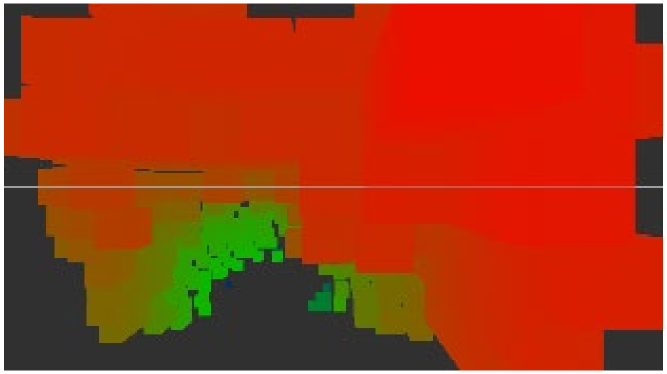
Cuboid Surface Representation: Cuboid provides a good view of the surroundings but requires a lot of vertices and triangles.	3,070	2,456	Good	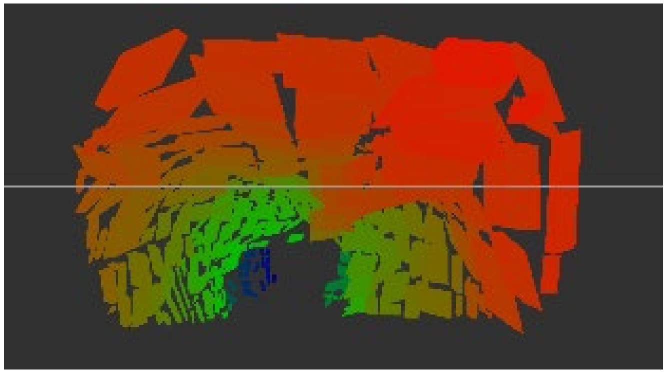
Ellipsoid Surface Representation: Ellipse representation has the best fidelity (note the hanging pipes clearly visible in the upper right) but requires a lot of vertices and triangles.	9,600	5,760	Excellent	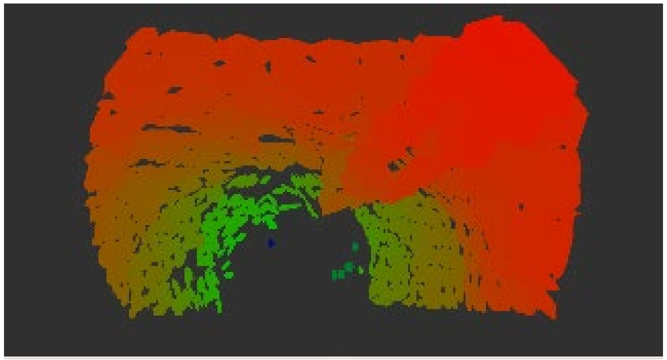

In addition to the various types of representations available, there are additional visualization capabilities and limitations to consider in the design process. According to the specifications listed in the Intel RealSense lidar camera range, the range is approximately 9 meters or 30 feet[42]. However, utilizing a different sensor could potentially extend the range. It is important to note that increasing the visualized range may have an impact on the tunneling effect, potentially decreasing the user's perception and overall understanding of the visuals. During internal testing, the depth colors were found to be optimal based on the current tunnel size and sensor configuration. However, it is possible to programmatically adjust the range and colors as desired using Unity.

After choosing the visualization method and building the application into HoloLens, the proposed system is tested in an experimental underground mine called Edgar Mine, located in Idaho Springs, Colorado. The final run snapshots are given in Figure 6 that shows the user perspective.

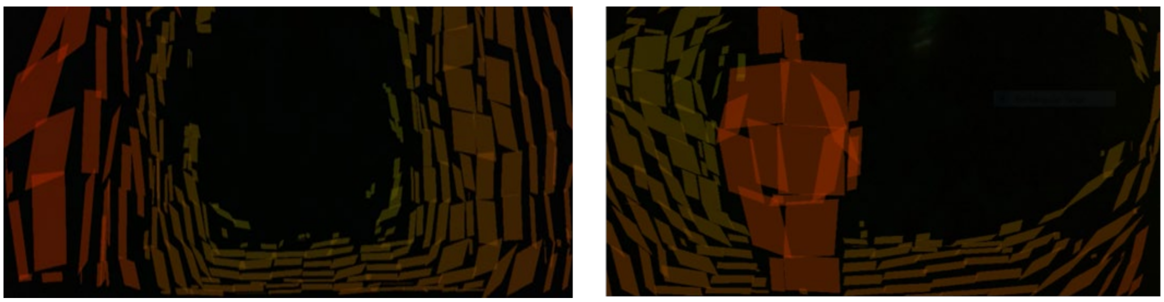

Figure6: Example snapshot of the enhancement

Finally, it is worth mentioning that the current configuration is capable of operating continuously for over an hour without requiring a recharge. It is important to note that the visualizations have a refresh rate of 50 Hz, which has been optimized to prevent any lag when the user makes sudden movements (e.g.; walking bristly, jumping and sudden head shake). Although the maximum refresh rate for HoloLens is 60 Hz, increasing it to this level does not result in a significant improvement in perception and instead reduces battery life. Current configuration and tests are done with cable connections for both data and power use. The system might require design modifications to provide a permissible system acceptable for use in mine rescue operations. Such as using this type of batteries might not be allowed in coal mines.

5.0 Publication Record and Dissemination Efforts

Conference: SPIE AR | VR | MR 2024 (Accepted as conference proceeding) *Underground mine emergency evacuation planning: AR implementation and case study:* Doga *Cagdas* Demirkan, Ava Segal, Abhidipta Mallik, Sebnem Duzgun, Andrew J. Petruska,

Conference: SME Mine Exchange 24 (Accepted as conference proceeding)

Using AR assistance in mine rescue, Doga Cagdas Demirkan, Ava Segal, Abhidipta Mallik, Sebnem Duzgun, Andrew J. Petruska,

Journal: AI, Computer Science and Robotics Technology, Special issues: SEARCH AND RESCUE ROBOTICS (Under Review) *Real-time perception enhancement in obscured environments for underground mine search and rescue teams* Doga Cagdas Demirkan, Ava Segal, Abhidipta Mallik, Sebnem Duzgun, Andrew J. Petruska,

Journal: Mining, Metallurgy & Exploration - Springer (In Process)

Journal: Lukas Fahle and Elizabeth A Holley and Gabriel Walton and Andrew J. Petruska and Jurgen F Brune. "Analysis of SLAM-based Lidar Data Quality Metrics for Geotechnical Underground Monitoring.", Mining, Metallurgy & Exploration, 2022

Journal: Lukas Fahle and Andrew J. Petruska and Gabriel Walton and Jurgen F. Brune and Elizabeth A. Holley, "Development and Testing of Octree-Based Intra-Voxel Statistical Inference to Enable Real-Time Geotechnical Monitoring of Large-Scale Underground Spaces with Mobile Laser Scanning Data", Remote Sensing, 2023

Invited Talk: NIOSH - Mine AutomationCommunity of Practice (CoP), Augmented Reality for Search and Rescue in the Underground: Challenges and Opportunities, September 2021

Invited Talk: Rootics & Automation In Mining Breakfast Series (Denver), Augmented Reality for Search and Rescue in the Underground: Challenges and Opportunities, October 2021

6.0 Conclusions and Impact Assessment

In this work, we combined a thermal imaging camera with a LiDAR sensor and visualized a real-time world construction as an AR interface. Our proposed methodology yielded a proof of concept wearable device for underground mine search and rescue personnel. The feasibility and progressive nature of the device were tested in an experimental underground mine located in Idaho Springs, Colorado. The results showed that combining the technologies we used enables faster, safer, and more effective disaster response for mine rescue operations. Not only does it allow the responders to search the environment more rapidly, but it also enables them to detect unexpected hazards before they become imminent threats. Moreover, the utility of the developed system is far-reaching, for example, for first responders searching smoke-filed burning structures. In the future, it might also enable autonomous systems to navigate these occluded environments effectively and enable disaster response to focus on the rescue in search-and-rescue.

While testing the end product, a few challenges were encountered. The first challenge was that, although the sensors and hard hat had fixed dimensions, the users' head size and eye distance to the sensors were different. This made a small offset for the visual enhancement interface. Since the search and rescue operations are time-critical, we added a wireless gaming controller for real-time alignment for the visual enhancement stream. The alignment helped users to fit the enhancement in four degrees of freedom.

The second challenge was that the HoloLens was not initially intended for dark environments, as the Microsoft software ceased to function as soon as the ambient lighting faded. As a workaround, the system allows the programmers to completely turn-off Microsoft provided tracking and rendering, which allows us to use the device at a lower level and project the images even if the HoloLense loses internal tracking.

Lastly, for collecting test and debug information, the application needs to be run in Unity. To do this, we used an open-source library for Unity called ROS-sharp [43]. Using a network bridge, a Unity program could then subscribe to ROS topics and collect the transmitted data. This results in a 3-way communication (LiDAR->Linux ROS network->Windows). This was not a significant issue as in the end, we would still have a 3-way communication of sensors communicating to ROS and that to the HoloLens. Furthermore, there was no visible change in the speed of visualizing a scene with moving objects (e.g., waving an arm, or walking around).

7.0 Recommendations for Future Work

Although the initial tests are done with the research team, more comprehensive human subject study is needed for statistically significant conclusions for evacuation and search and rescue missions.

Lastly, with the technological advancements such as battery life and capacity, sensor weight and compatibility such as Radar, and faster processing power might excel our platform by making it more light weight and durable.

8.0 References

1. Chen J, Li S, Liu D, Li X. Airobsim: Simulating a multisensor aerial robot for urban search and rescue operation and training. Sensors (Switzerland). 2020;20(18):1–20.

2. Beerbower D, Energy P, Biggerstaff R, Coal A, Blackwell WK, Energy C, et al. Mine Rescue Handbook.

3. Bertrand JWM, Fransoo JC. Modelling and simulation. Research Methods for Operations Management. 2016. 290–330 p.

4. Zlot R, Bosse M. Efficient Large-Scale 3D Mobile Mapping and Surface Reconstruction of an Underground Mine. In: Yoshida K, Tadokoro S, editors. Field and Service Robotics: Results of the 8th International Conference [Internet]. Berlin, Heidelberg: Springer Berlin Heidelberg; 2014. p. 479–93. Available from: https://doi.org/10.1007/978-3-642-40686-7_32

5. Conti RS, Chasko LL, Wiehagen WJ, Lazzara CP. Fire Response Preparedness for Underground Mines. Inf Circ 9481 [Internet]. 2005;25. Available from: https://www.cdc.gov/niosh/mining/UserFiles/works/pdfs/2006-105.pdf

6. Zimroz P, Trybała P, Wróblewski A, Góralczyk M, Szrek J, Wójcik A, et al. Application of UAV in search and rescue actions in underground mine—A specific sound detection in noisy acoustic signal. Energies. 2021;14(13):1–21.

7. Willette K. First Responder. NFPA J [Internet]. 2018; Available from: https://www.nfpa.org/News-and-Research/Publications-and-media/NFPA-Journal/2018/January-February-2018/Columns/First-Responder

8. Wang W, Dong W, Su Y, Wu D, Du Z. Development of Search-and-rescue Robots for Underground Coal Mine Applications. J F Robot. 2014;31(3):386–407.

9. Nüchter A, Surmann H, Lingemann K, Hertzberg J, Thrun S. 6D SLAM with an application in autonomous mine mapping. Proc - IEEE Int Conf Robot Autom. 2004;2004(2):1998–2003.

10. Rogers JG, Schang A, Nieto-Granda C, Ware J, Carter J, Fink J, et al. The DARPA SubT Urban Circuit Mapping Dataset and Evaluation Metric. In: Siciliano B, Laschi C, Khatib O, editors. Experimental Robotics. Cham: Springer International Publishing; 2021. p. 391–401.

11. Thrun S. Probabilistic robotics. Commun ACM. 2002;45(3):52–7.

12. Wang G, Wang W, Ding P, Liu Y, Wang H, Fan Z, et al. Development of a search and rescue robot system for the underground building environment. J F Robot. 2023;40(3):655–83.

13. Li S, Guo T, Mo R, Zhao X, Zhou F, Liu W, et al. A rescue-assistance navigation method by using the underground location of WSN after disasters. Sensors (Switzerland). 2020;20(8):1–25.

14. Ackerman E. Robots Conquer the Underground: What Darpa's Subterranean Challenge Means for the Future of Autonomous Robots. IEEE Spectr. 2022;59(5):30–7.

15. Petrlik M, Petráček P, Krátký V, Musil T, Stasinchuk Y, Vrba M, et al. UAVs Beneath the Surface: Cooperative Autonomy for Subterranean Search and Rescue in DARPA SubT. F Robot. 2023;3(1):1–68.

16. Leslie M. Robots Tackle DARPA Underground Challenge. Engineering [Internet]. 2022;13:2–4. Available from: https://doi.org/10.1016/j.eng.2022.04.003
17. DEMIRKAN DC, Duzgun S. An Evaluation of AR-Assisted Navigation for Search and Rescue in Underground Spaces. In: 2020 IEEE International Symposium on Mixed and Augmented Reality Adjunct (ISMAR-Adjunct). 2020. p. 1–2.
18. Bertin J. Semiologie graphique. Paris; 1967.
19. Bertin J. Semiology of Graphics: Diagrams, Networks, Maps. UMI Research Press; 1983. 429 p.
20. MacEachren AM. Some Truth With Maps: A Primer on Symbolization and Design. Association of American Geographers; 1994. 129 p.
21. Wolfe JM. Guided Search 2.0 A revised model of visual search. Psychon Bull Rev. 1994;1(2):202–38.
22. Zhang ZP, Liu J. Research on the symbol vision variable of the three-dimension virtual battle environment. Geomatics Spat Inf Technol. 2014;37(9):7–9.
23. Hong S, Mao B, Li B. Preliminary Exploration of Three-Dimensional Visual Variables in Virtual Reality. In: 2018 International Conference on Virtual Reality and Visualization (ICVRV). IEEE; 2018. p. 28–34.
24. Conferance Ranks. No Title [Internet]. Available from: http://www.conferenceranks.com/index.html?searchall=Human+Factors+in+Computing+Systems#data
25. Ens B, Bach B, Cordeil M, Engelke U, Serrano M, Willett W, et al. Grand Challenges in Immersive Analytics. 2021;17:1–17. Available from: http://hdl.handle.net/1880/112984
26. Dasgupta A, Poco J, Wei Y, Cook R, Bertini E, Silva CT. Bridging Theory with Practice: An Exploratory Study of Visualization Use and Design for Climate Model Comparison. IEEE Trans Vis Comput Graph. 2015;21(9):996–1014.
27. Laha B, Sensharma K, Schiffbauer JD, Bowman DA. Effects of immersion on visual analysis of volume data. IEEE Trans Vis Comput Graph. 2012;18(4):597–606.
28. Adams H, Stefanucci J, Creem-Regehr S, Bodenheimer B. Depth Perception in Augmented Reality: The Effects of Display, Shadow, and Position. Proc - 2022 IEEE Conf Virtual Real 3D User Interfaces, VR 2022. 2022;792–801.
29. Arjun S, Reddy GSR, Mukhopadhyay A, Vinod S, Biswas P. Evaluating Visual Variables in a Virtual Reality Environment. 34th Br Hum Comput Interact Conf Interact Conf BCS HCI 2021. 2021;133–8.
30. Koch C, Ullman S. Shifts in selctive visual attention: twords the underlying neural circuitry. Hum Neurobiol. 1985;4(10):219–27.
31. Itti L, Koch C, Niebur E. A Model of Saliency-Based Visual Attention for Rapid Scene Analysis. IEEE Trans Pattern Anal Mach Intell. 1998;20(11):1254–9.
32. Niebur E, Koch C. Control of selective visual attention: modeling the {``}where{''} pathway. Adv Neural Inf Process Syst. 1996;8.
33. Veale R, Hafed ZM, Yoshida M. How is visual salience computed in the brain? Insights

from behaviour, neurobiology and modeling. Philos Trans R Soc B Biol Sci. 2017;372(1714).

34. Itti L, Koch C. Computational Modelling of. Neuroscience [Internet]. 2001;2(February):1–11. Available from: http://www.psypress.com/computational-modelling-9781841698557

35. Huy THN, Carlon MKJ, Cross JS. Simulated Gaze Tracking using Computer Vision for Virtual Reality. Proc 2022 8th Int Conf Immersive Learn Res Network, iLRN 2022. 2022;1–5.

36. Arvanitis G, Lalos AS, Moustakas K. Saliency mapping for processing 3D Meshes in industrial modeling applications. IEEE Int Conf Ind Informatics. 2019;2019-July:683–6.

37. Hosseinkhani J, Joslin C. Significance of Bottom-Up Attributes in Video Saliency Detection without Cognitive Bias. In: 2018 IEEE 17th International Conference on Cognitive Informatics & Cognitive Computing (ICCI*CC). 2018. p. 606–13.

38. Wang Y, Su H, Zhang B, Hu X. Learning Reliable Visual Saliency For Model Explanations. IEEE Trans Multimed. 2020;22(7):1796–807.

39. Bruce NDB, Tsotsos JK. Saliency based on information maximization. Adv Neural Inf Process Syst. 2005;155–62.

40. Duzgun S, Isleyen E, Demirkan D ~C., Orsvuran R, Bozdag E, Pugmire D. Virtual and Augmented Reality for Visualization of Big Data: Examples from Deep Earth to Subsurface. In: AGU Fall Meeting Abstracts. 2019. p. IN21B-05.

41. Rusu RB, Cousins S. 3D is here: Point Cloud Library (PCL). In: IEEE International Conference on Robotics and Automation (ICRA). Shanghai, China; 2011.

42. Intel. Intel® RealSense™ LiDAR Camera L515 [Internet]. Available from: https://store.intelrealsense.com/buy-intel-realsense-lidar-camera-l515.html#tech-specs

43. Bischoff M. ROS# [Internet]. GitHub; 2019. Available from: https://github.com/siemens/ros-sharp/releases/tag/v1.5

9.0 Appendices

Appendix A: Post Survey Questions

NASA Task Load Index

Hart and Staveland's NASA Task Load Index (TLX) method assesses work load on five 7-point scales. Increments of high, medium and low estimates for each point result in 21 gradations on the scales.

Name	Task	Date

Mental Demand — How mentally demanding was the task?

Very Low — Very High

Physical Demand — How physically demanding was the task?

Very Low — Very High

Temporal Demand — How hurried or rushed was the pace of the task?

Very Low — Very High

Performance — How successful were you in accomplishing what you were asked to do?

Perfect — Failure

Effort — How hard did you have to work to accomplish your level of performance?

Very Low — Very High

Frustration — How insecure, discouraged, irritated, stressed, and annoyed wereyou?

Very Low — Very High